

## Self-Organized Ureido Substituted Diacetylenic Organogel. Photopolymerization of One-Dimensional Supramolecular Assemblies to Give Conjugated Nanofibers

Olivier J. Dautel,\* Mike Robitzer, Jean-Pierre Lère-Porte, Françoise Serein-Spirau, and Joël J. E. Moreau\*

Contribution from the Hétérochimie Moléculaire et Macromoléculaire UMR CNRS 5076, Ecole Nationale Supérieure de Chimie de Montpellier, 8 rue de l'Ecole Normale 34296 Montpellier Cedex 05, France

Received July 28, 2006; E-mail: joel.moreau@enscm.fr; olivier.dautel@enscm.fr

**Abstract:** The introduction of the urea function as structure directing agent of diacetylene organogels (DA-OGs) has been achieved. Despite the urea function being one of the most frequently used structure directing agents for the formation of organogels, it has never been exploited in the fabrication and photopolymerization of DA-OGs. The self-association of ureas involving two hydrogen bonds is much stronger than that of urethanes or amides, and the resulting supramolecular assemblies are completely insoluble. In this context, 1,1'-(hexa-2,4-diyne-1,6-diyl)bis(3-(10-(triethoxysilyl)decyl)urea) **2** was synthesized. Compound **2** was soluble owing to the triethoxysilane function that we recently used in the fabrication of a silylated bis-urea-stilbene organogel. It formed an organogel, and its photopolymerization was studied in cyclohexane. The loss of the gel state and the formation of a red solution resulting from the polymerization were found to be the result of the constraints introduced by the urea function in close vicinity to the polymerizable function. To obtain an ureido substituted diacetylenic organogelator affording a blue highly conjugated polydiacetylene (PDA) without a sol–gel transition, a propylene spacer was introduced to move the urea function away from the polymerizable function (derivative **3**). The thermochromism exhibited by the latter in the solid state was studied. Using the same setup and the same sample, UV–vis and FTIR spectra were simultaneously recorded as a function of the temperature to highlight a relation between color changes and urea association mode changes. The data showed that the reversible thermochromic transition must be associated with a reversible supramolecular modification and, conversely, that irreversible chromic transitions are the result of irreversible structural modifications. The chromic effects of the acidic hydrolysis–polycondensation of the trialkoxysilyl groups to form a siloxane network were studied on a thin film of **3**. In the same way, solvent effects on the color of the organogels of **3** were also investigated. Correlations could be established between the different stimuli. These results provide a deeper understanding of the precise molecular mechanism of the blue to red transition and of the reversibility of the purple to red transition generally encountered in PDA thermochromism.

### Introduction

Recently, diacetylene organogels (DA-OGs) have attracted much interest because their noncovalently organized fibrous networks can be photopolymerized through 1,4-addition reactions of the diyne groups, giving stable covalently linked polydiacetylene networks.<sup>1</sup> To date, however, only a few papers describing diacetylene gels have been reported, including rather sophisticated self-associated compounds through van der Waals interactions<sup>2</sup> or through hydrogen-bonded urethane<sup>3</sup> or amide<sup>4</sup> derivatives.

The urea function is certainly one of the most frequently used structure directing agents. The hydrogen-bond pattern resulting

from its association is well-described and drives the molecular assemblies to one-dimensional objects, a requirement in organogel formation.<sup>5,6</sup> Ureido substituted diacetylenic compounds

- (1) Cantow, H.-J. *Polydiacetylenes*; Springer-Verlag: Berlin, 1984.
- (2) (a) Wang, G.; Hollingsworth, R. I. *Adv. Mater.* **2000**, *12*, 871–874. (b) George, M.; Weiss, R. G. *Chem. Mater.* **2003**, *15*, 2879–2888.
- (3) (a) Tamaoki, N.; Shimada, S.; Okada, Y.; Belaisaoui, A.; Kruk, G.; Yase, K.; Matsuda, H. *Langmuir* **2000**, *16*, 7545–7547. (b) Nagasawa, J.; Kudo, M.; Hayashi, S.; Tamaoki, N. *Langmuir* **2004**, *20*, 7907–7916.

- (4) (a) Masuda, M.; Hanada, T.; Yase, K.; Shimizu, T. *Macromolecules* **1998**, *31*, 9403–9405. (b) Inoue, K.; Ono, Y.; Kanekiyo, Y.; Hanabusa, K.; Shinkai, S. *Chem. Lett.* **1999**, 429–430. (c) Masuda, M.; Hanada, T.; Okada, Y.; Yase, K.; Shimizu, T. *Macromolecules* **2000**, *33*, 9233–9238. (d) Miyawaki, K.; Harada, A.; Takagi, T.; Shibakami, M. *Synlett* **2003**, 349–352. (e) Aoki, K.; Kudo, M.; Tamaoki, N. *Org. Lett.* **2004**, *6*, 4009–4012. (f) Shirakawa, M.; Fujita, N.; Shinkai, S. *J. Am. Chem. Soc.* **2005**, *127*, 4164–4165.
- (5) (a) Scoonbeek, F. S.; van Esch, J. H.; Wegewijs, B.; Rep, D. B. A.; de Haas, M. P.; Klapwijk, T. M.; Kellogg, R. M.; Feringa, B. L. *Angew. Chem., Int. Ed.* **1999**, *38*, 1393–1397. (b) Jung, J. H.; Ono, Y.; Shinkai, S. *Chem. Eur. J.* **2000**, *24*, 4552–4557. (c) George, M.; Tan, G.; John, V. T.; Weiss, R. G. *Chem. Eur. J.* **2005**, *11*, 3243–3254. (d) Vos, M. R. J.; Jardl, G. E.; Pallas, A. L.; Breurken, M.; van Asselen, O. L. J.; Bomans, P. H. H.; Leclère, P. E. L. G.; Frederik, P. M.; Nolte, R. J. M.; Sommerdijk, N. A. J. M. *J. Am. Chem. Soc.* **2005**, *127*, 16768–16769.
- (6) Specific examples related to comparable compounds: (a) Varghese, R.; George, S. J.; Ajayaghosh, A. *Chem. Commun.* **2005**, 593–594. (b) Xiaoping Nie, X.; Wang, G. *J. Org. Chem.* **2006**, *71*, 4734–4742. (c) Würthner, F.; Hanke, B.; Lyssetska, M.; Lambright, G.; Harms, G. S. *Org. Lett.* **2005**, *7*, 967–970.

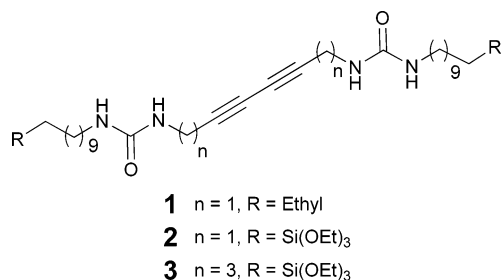


**Figure 1.** New ureido substituted diacetylenic derivatives.

have been patented as acid complexed acetylenic derivatives useful as environmental indicating devices.<sup>7</sup> Moreover, Koevoets et al. have also combined urea units with diacetylene groups to fabricate highly extensible copolyether ureas with cross-polymerizable diacetylene hard blocks.<sup>8</sup> However, the urea function has never been exploited in the fabrication and the photopolymerization of diacetylene organogels.

In this paper, we investigated the relationships between chemical structures and behavior during gelation and subsequent topochemical polymerization using novel ureido substituted diacetylenic derivatives with very simple structures (Figure 1). Here, we describe detailed studies on these compounds with respect to their gelling ability, hydrogen bonding (jointly monitored by UV-vis and Infrared spectroscopies), and thermochromism mechanisms. We report here the first example of a remarkable effect that the alkylene spacer length ( $n$ ) has on the length of the resulting nano-objects from the photopolymerized organogels.

For this study, we prepared a series of diacetylene derivatives (1–3) through condensation between isocyanates and diacetylenediamines in tetrahydrofuran (THF). Compounds 1 and 2 have the same alkylene spacer ( $n = 1$ ) but different end chains. The presence of aliphatic side chains in 1–3 should reinforce the self-association properties of the urea function through collective noncovalent van der Waals interactions but could also reduce the precursor solubility. Indeed, the self-association of ureas involving two hydrogen bonds is much stronger than that of urethanes or amides, the resulting supramolecular materials being often extremely insoluble. The high temperature, necessary to solubilize them, could produce premature polymerization of the diacetylenic moiety.<sup>7</sup> To overcome this, we explored two approaches. First, our strategy for introducing solubility to the DA-OGs precursor was to take advantage of the triethoxysilane function ( $\text{Si}(\text{OEt})_3$ ) that we recently used in the fabrication of the silylated bis-urea-stilbene organogel used as a sol-gel processable silicate precursor.<sup>9</sup> The steric hindrance and the lipophilicity introduced by this function should increase the solubility of the compounds. To that purpose, 2, containing triethoxysilane end groups, was synthesized. Second, the rigidity of the hydrogen-bonded urea function close to the polymerizable fragment may inhibit the polymerization. The constraints introduced by hydrogen-bonding patterns were tuned by the introduction of a propylene spacer in the synthesis of 3. The urea function was moved away from the polymerizable function

while keeping the necessary odd number of  $\text{CH}_2$  groups ( $n = 3$ ) to obtain the favorable geometry for photopolymerization (see Supporting Information).<sup>10</sup>

## Results and Discussion

**Synthesis of Ureido Substituted Diacetylenic Organogelators.** In a first approach, the synthesis of the precursor 1 was achieved by the condensation of 2.5 equiv of dodecylisocyanate and 1 equiv of hexa-2,4-diyne-1,6-diamine<sup>11</sup> in dry THF (10 mL) (Scheme 1). The mixture was heated at 50 °C for 3 h. After cooling to room temperature, the reaction mixture was concentrated under reduced pressure to give a white solid. Compound 1 was suspended in dry pentane (20 mL) and filtered to yield 85% of 1 as a white solid that turned purple on standing in daylight. Compound 1 was insoluble even in DMSO. Attempts to obtain organogels from compound 1 irremediably resulted in premature polymerization of the diacetylenic moieties as shown by the purple coloration of the suspension.

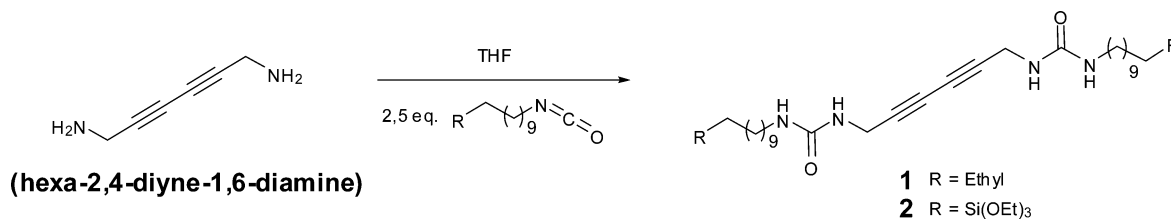
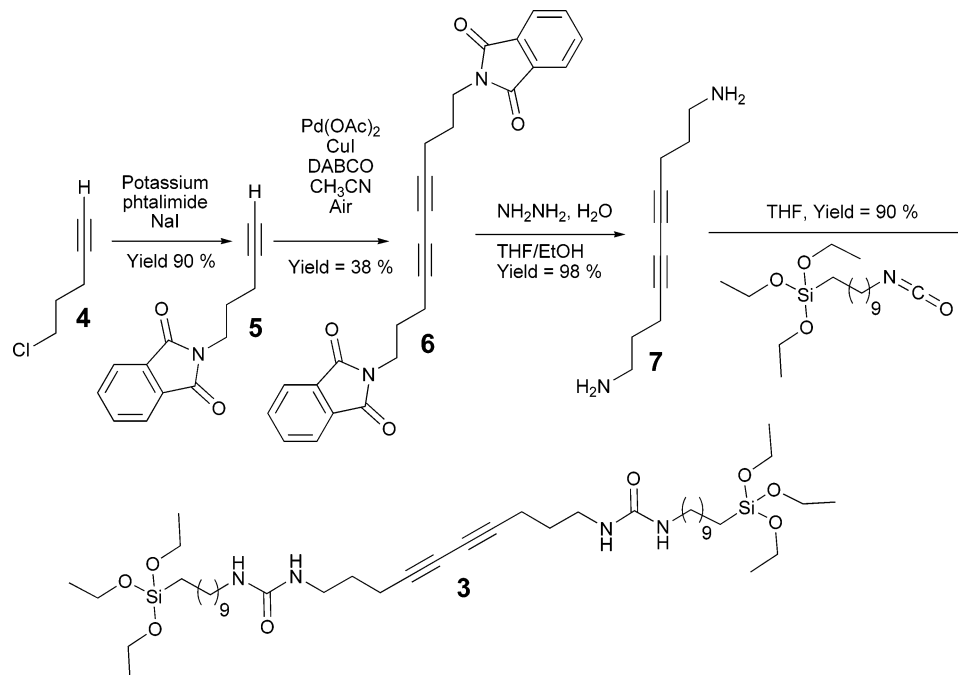
In this context, the diacetylenic silane 2 was synthesized following the same procedure as for 1 from the condensation of 2.5 equiv of the triethoxy(10-isocyanatododecyl)silane<sup>12</sup> and hexa-2,4-diyne-1,6-diamine. As expected, 2 was highly soluble in most organic solvents owing to the steric hindrance and the lipophilicity introduced by the triethoxysilane functions.

The synthetic path to 3 involves the synthesis of deca-4,6-diyne-1,10-diamine 7 to incorporate the desired propylene spacer ( $n = 3$ ). Usually, symmetric bisacetylenes are obtained from the oxidative coupling of terminal alkynes following Glaser-Hay coupling.<sup>13</sup> In this case, we found that the use of the catalytic copper(I)-TMEDA complex, which is reoxidized in the catalytic cycle by oxygen bubbling, was quite capricious and hazardous. Therefore, the organogelator 3 was synthesized by the quite novel and efficient Pd(II)-catalyzed homocoupling reaction of the terminal alkyne 5 in air (Scheme 2).<sup>14</sup> Compound 5 was synthesized by the Gabriel synthesis of the primary amine.<sup>15</sup>

**Study of the Organogels.** Compound 2 gelatinizes toluene, THF, and even nonpolar hydrophobic cyclohexane at concentrations as low as 0.1 wt %. To our knowledge, this compound is one of the most powerful organogelators. Cyclohexane was the solvent chosen for the organogels studies for two major reasons: (i) it does not absorb UV-vis radiation at 254 nm, and this optical property is essential for the photopolymerization of the diyne subunits and (ii) its boiling point (81 °C) is adequate to give the required energy for breaking the hydrogen-bond system of the urea function. 2 mg/mL (0.25 wt %) of 2, dissolved in hot cyclohexane and allowed to stand at room temperature, gives a colorless translucent organogel (Figure 2, inset) with a sol-gel phase transition temperature ( $T_{\text{gel}}$ ) of 57

(7) (a) Preziosi, A. F.; Prusik, T. U.S. Patent 4,789,636, 1988. (b) Preziosi, A. F.; Prusik, T. U.S. Patent 4,788,151, 1988.  
 (8) Koevoets, R. A.; Sijbesma, R. P.; Magusin, P. C. M. M.; Meijer, E. W. *Polym. Prepr.* **2003**, *44* (2), 199–200.  
 (9) Dautel, O. J.; Lère-Porte, J. P.; Moreau, J. J. E.; Wong Chi Man, M. J. *Chem. Soc., Chem. Commun.* **2003**, 2662.

(10) (a) Jenkins, S.; Jacob, K. I.; Kumar, S. *J. Mol. Struct.* **2000**, *525*, 277–286. (b) Aoki, K.; Kudo, M.; Tamaoki, N. *Org. Lett.* **2004**, *6*, 4009–4012.  
 (11) Kato, J.; Nakamura, K. Japanese patent 62267248, 1987.  
 (12) Joly, P.; Ardes-Guisot, N.; Kar, S.; Granier, M.; Durand, J.-O.; Melynk, O. *Eur. J. Org. Chem.* **2005**, *12*, 2473–2480.  
 (13) For a review see: Siemsen, P.; Livingston, R. C.; Diederich, F. *Angew. Chem.* **2000**, *112*, 2740–2767. *Ibid.*, *Angew. Chem., Int. Ed.* **2000**, *39*, 2632–2657.  
 (14) Li, J.-H.; Liang, Y.; Xie, Y.-X. *J. Org. Chem.* **2005**, *70*, 4393–4396.  
 (15) Bellier, B.; Dugave, C.; Etivant, F.; Genet, R.; Gigoux, V.; Garbay, C. *Bioorg. Med. Chem. Lett.* **2004**, *14*, 369–372.

**Scheme 1.** Synthesis of New Bis-ureas Derived from Hexa-2,4-diyne-1,6-diamine**Scheme 2.** Synthesis of New Bis-urea Diacetylenic Organogelator **3**

°C determined using the ball method.<sup>16</sup> The sol–gel transition was studied as a function of the gel concentration. The  $T_{\text{gel}}$  values increased linearly with concentrations in the 0.1–0.7 wt % range and then became independent of concentrations up to at least 1 wt %: in these last conditions, the  $T_{\text{gel}}$  was 68 °C.<sup>17</sup> This behavior is commonly observed for organogels.<sup>18</sup>

The hydrogen-bond pattern of the urea enabled the sol–gel transition to be followed by monitoring the Fourier Transform Infrared (FTIR) behavior of the organogel as a function of the temperature. Indeed, it can be described by the two symmetrical hydrogen bonds between the carbonyl function of one urea moiety and the secondary amines of another vicinal urea molecule (cf. Figure 2). A urea function is characterized by three infrared absorption bands corresponding to the N–H stretch ( $\nu_{\text{NH}} \approx 3336 \text{ cm}^{-1}$ ), the C=O stretch called the Amide I band ( $\nu_{\text{CO}} \approx 1623 \text{ cm}^{-1}$ ), and a combination of the N–H deformation and the C–N stretch called the Amide II band ( $\delta_{\text{NH}} + \nu_{\text{CN}} \approx 1584 \text{ cm}^{-1}$ ). The intensities and wavenumbers of those three bands are directly related to the hydrogen-bond strength of the system.<sup>19</sup> In the case of a transition from an associated urea to

a free urea, the Amide I band is shifted to higher wavenumbers and the Amide II band to lower wavenumbers.

In this context, a 2 mg/mL cyclohexane gel of **2** was introduced in a KBr sealed cell, and the FTIR spectra were recorded at different temperatures (Figure 2, setup described in Supporting Information). At room temperature, the Amide I and the Amide II bands, found, respectively, at 1623 and 1584  $\text{cm}^{-1}$ , are representative of an associated urea function. Upon increasing the temperature, the intensity of the two bands was lowered, and two new bands appeared at 1645 and 1567  $\text{cm}^{-1}$ . The occurrence of two isobestic points at 1637 and 1576  $\text{cm}^{-1}$  demonstrated the presence of one-mode association alternation of urea functions and of equilibrium between the free and the associated species. At  $\approx 65$ –70 °C, in the temperature range corresponding to the  $T_{\text{gelmax}}$  determined by the ball method, no more association between ureas is observed. This result shows that the lower  $T_{\text{gels}}$  ( $40 \text{ °C} < T_{\text{gels}} < 60 \text{ °C}$ ) observed at low concentrations of gelator are in fact due to the small number of fibers constituting the network. At these temperatures, the hydrogen bond is still effective, and the fibers are present, but the thermal motion of the fibers allowed the ball to cross the intermingled network. At higher concentrations, the network is so tightly intermingled that the ball can only drop with the breaking of the fibers by disruption of the hydrogen bonds. No thermal alteration or premature thermal reticulation of the triethoxysilane functions was observed (see Supporting Information).

- (16) (a) de Loos, M.; van Esch, J.; Stokroos, I.; Kellogg, R. M.; Feringa, B. L. *J. Am. Chem. Soc.* **1997**, *119*, 12675–12676. (b) Tan, H. M.; Moet, A.; Hiltner, A.; Baer, E. *Macromolecules* **1983**, *16*, 28–34. (c) Takahashi, A.; Sakai, M.; Kato, T. *Polym. J.* **1980**, *12*, 335–341.
- (17)  $T_{\text{gel}}$  values were determined using the ball method with a ball weighting 450 mg.  $T_{\text{gel}}$  maximum was obtained with a 1 wt % gel at 68 °C. See supporting Information.
- (18) Terech, P.; Weiss, R. G. *Chem. Rev.* **1997**, *97*, 3133–3160.
- (19) Jazyn, J.; Stockhauser, M.; Zywicki, B. *J. Phys. Chem.* **1987**, *91*, 754–757.

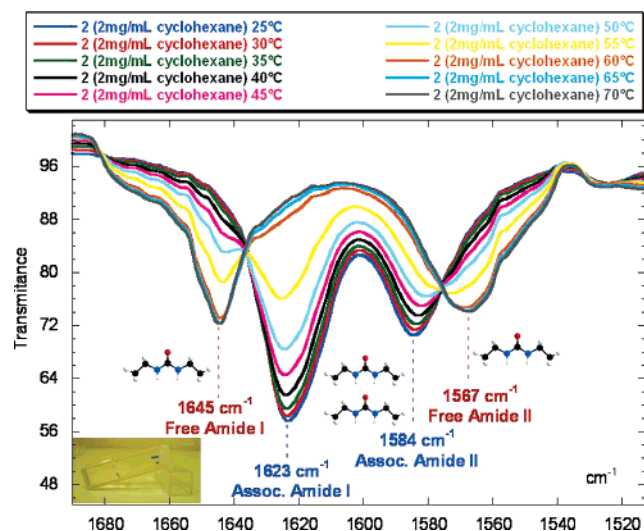


**Figure 2.** FTIR of a 2 mg/mL organogel of **2** in cyclohexane as a function of the temperature. (Inset: photograph of a 2 mg/mL organogel of **2** in cyclohexane).

Compound **3** is also highly soluble in most solvents. It gelatinizes toluene, THF, and cyclohexane at concentrations as low as 0.1 wt %. The 2 mg/mL (0.25 wt %) of **3**, dissolved in hot cyclohexane and allowed to stand at room temperature, furnishes a colorless translucent organogel (see Supporting Information) with a sol–gel phase transition temperature ( $T_{\text{gel}}$ ) of 78 °C determined using the ball method. The sol–gel transition was studied as a function of the gel concentration. The  $T_{\text{gel}}$  values increase linearly with concentrations in the 0.1–0.8 wt % range. At higher concentrations, the sol–gel transition was not observed below the boiling point of cyclohexane. The  $T_{\text{gelmax}}$  value was determined to be at 94 °C with the ball method, using tetrachloroethylene as a higher boiling point solvent. The increase in the  $T_{\text{gelmax}}$  from **2** to **3** is related to the introduction of the propylene spacer that increases the London forces and avoids all geometrical constraints of the urea function. In the same way, the FTIR analysis of the organogel, as a function of the temperature, showed that the sol–gel transition was around 100 °C and that no thermal alteration or premature thermal curing of the triethoxysilane functions was observed (see Supporting Information).

**Photopolymerization of the Organogels.** Photopolymerization of a 2 mg/mL cyclohexane gel of **2** by irradiation at 254 nm with a 6 W UV lamp at a distance of 10 cm for 30 min results in the loss of the gel state and in a red solution characterized by an absorption maximum at 515 nm (Figure 3). This result is surprising since the polymerization of DA-OGs, when it occurs, usually results in the reinforcement of the organogel.<sup>2–4</sup> The color of the resulting polydiacetylene organogels (PDA-OGs) depends mainly on the extension of the  $\pi$ -delocalization along the polymerized fibers. A PDA-OG will exhibit a red color in the case of constrained fibers generating low delocalization and a blue color in the case of a long-range delocalization.

The observed red color could be explained by the steric hindrance introduced by the triethoxysilane functions that may induce distortions along the fibers, but it does not explain the loss of the gel state. The irradiation at 254 nm for 30 min of **3** as a colorless translucent organogel (2 mg/mL) in cyclohexane provided a blue PDA-OG while retaining the gel state (Figure

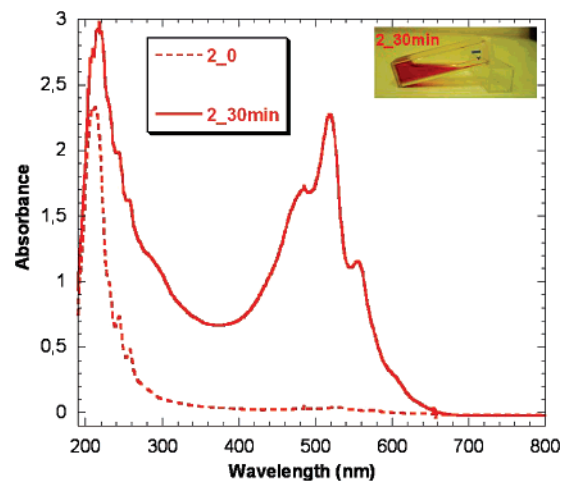


**Figure 3.** UV spectra of the organogel of **2** (2 mg/mL) in cyclohexane before (dotted line) and after 30 min of irradiation at 254 nm (full line). (Inset: photograph of a 2 mg/mL organogel of **2** irradiated in cyclohexane).

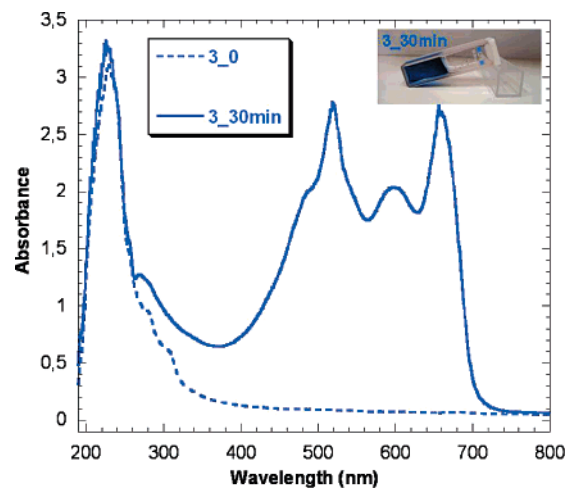


**Figure 4.** UV spectra of an organogel of **3** (2 mg/mL) in cyclohexane before (dotted line) and after 30 min of irradiation at 254 nm (full line). (Inset: photograph of a 2 mg/mL organogel of **3** irradiated in cyclohexane).

4). This observation confirms that the triethoxysilane function is not responsible for the loss of the gel state. This blue phase is characterized by an absorption maximum wavelength at 675 nm.

Further insight concerning the different supramolecular architectures was given by Atomic Force Microscopy (AFM) images of the cyclohexane organogels before and after irradiation. The irradiation was done in an UV cell, and gels were diluted 10-fold before being dropcast on a silicon wafer (Figure 5). Before irradiation, both organogelators (**2** and **3**) furnished very high quality fibers (Figure 5a,c). Their width ranged from 30 to 60 nm corresponding to  $-6$  to 12 parallels stacks of the organogelator (**2** or **3** length is  $\approx 5$  nm). Their average thickness is about 1 nm, and their length can reach tens of micrometers.

During irradiation of **2**, the constraints imposed by the urea close to the polymerizable function results in fragmentation of the fibers into nanorods (30 nm wide and 300 nm long, Figure 5b). Conversely, the  $-(\text{CH}_2)_3-$  spacer, introduced between the urea and the diacetylene in **3**, avoids breaking the fibers that



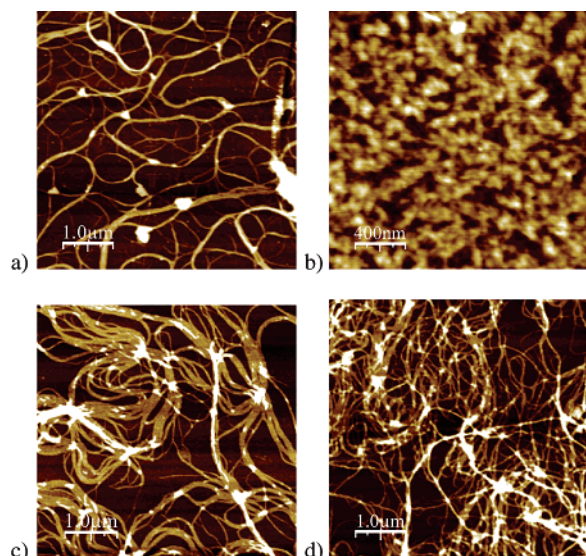


**Figure 5.** Organogel of **2** (2 mg/mL in cyclohexane) diluted 10-fold: (a) before irradiation and (b) after 30 min irradiation and **3** (2 mg/mL in cyclohexane) diluted 10-fold: (c) before irradiation and (d) after 30 min irradiation.

remain during and after irradiation; thus, this propylene spacer enables the design of highly  $\pi$ -conjugated blue fibers (Figure 5d).

We have therefore demonstrated the synthesis and photopolymerization of the first diacetylene organogels using urea as the structure directing agent. From these results, it is clear that the urea function, in the case of the PDA-OG, offers the possibility of tuning the size of the objects according to the constraints brought by the urea hydrogen-bonding pattern. Solubility enhancement from the triethoxysilane function could be generalized to all otherwise useless insoluble urea derivatives. We believe that a simple trialkylsilyl group could play this role, but the triethoxysilane function also exhibits a curable activity useful in materials science.

**Relation between Color Changes and Urea Association Mode Changes: Thermochromism, Solvatochromism, and Acidochromism.** It is now well-established that PDAs are thermochromic materials. This property was recently illustrated by Peng et al.<sup>20</sup> in the case of bulk silicate materials. In this context, **3** was evaluated as a thermochromatically responsive material.

A 2 mg/mL cyclohexane colorless organogel of **3** dropcast on a quartz plate was irradiated at 254 nm for 5 min to exhibit a blue color. Upon heating, the quartz plate showed three different chromatic transitions from blue to red with an intermediate purple coloration (Figure 6a). Unlike the blue to purple transition, the purple to red transition was reversible. In a first approach, the three different colors were characterized by means of the UV-vis spectra for the 2 mg/mL cyclohexane colorless organogel of **3** dropcast on a quartz plate and irradiated at 254 nm for 5 min. The blue phase was characterized by an absorption maximum at 675 nm (Figure 6b, blue line), the red phase by a maximum at 532 nm (Figure 6b, red line), and the purple phase exhibited an intermediate spectrum (Figure 6b, purple line). A first observation must be stressed: the blue

phases obtained in the gel state and in the solid state are spectroscopically different. Indeed, the UV-vis spectrum characterizing the blue phase obtained in the solid state (Figure 6b, blue line) exhibits only one major absorption band with a maximum wavelength of 675 nm. In this case, it is a pure blue phase. Conversely, the spectrum characterizing the blue phase obtained from the organogel (Figure 4, blue line) exhibits two major absorption bands with two maxima at 675 nm but also a red contribution at 515 nm. This red contribution in the PDA-OG originates probably from very small soluble supramolecular assemblies that do not contribute to the gel formation but can be polymerized and produce the poorly conjugated red PDA. Those nano-objects do not appear in the solid state because of the increase of concentration during the dewetting of the dropcast organogel layer.

This case of color change is different from the precedent example where the red and blue colors were due to two different sizes of nano-objects. In this latter case, the color of the resulting polydiacetylene depends mainly of the extension of the  $\pi$ -delocalization along the polymerized fibers. The color changes could be followed with the naked eye, but transition temperatures were precisely determined by the means of UV spectroscopy as a function of the temperature (Figure 7).

The precise molecular mechanism of the blue to red transitions is not completely understood. In the same way, no information on the reversibility of the purple to red transition is available. Numerous investigations on color transitions have relied on data obtained from employing one or two spectroscopic techniques, typically visible absorption<sup>21,22</sup> and resonance Raman spectroscopy.<sup>23,26</sup> These techniques directly probe the polymerized ene-yne chromophoric unit but not the pendent side chain conformation. Other methods such as <sup>13</sup>C NMR<sup>27,28</sup> can elucidate the pendent chain structure. However, the assignment of specific conformational changes requires the use of a synthetic model with a well-known conformation.<sup>29</sup> Taken as a whole, the embodied work on PDA thermochromism suggests two basic threads: (i) the blue to red thermochromic transition is associated with the reduction of the effective conjugated length of the ene-yne backbone and (ii) the electronic properties of the polymer ene-yne backbone are strongly coupled to pendent side chain conformation. However, many conflicting reports exist, and general principles and rules have yet to be established.<sup>30,31</sup> A few reports in the literature have proposed that the side chain entanglement and disordering directly affect the backbone conjugation.<sup>22–24</sup> A more detailed and direct molecular level probe of side chain group structure during the color transition is desirable to elucidate these effects. In the present case, FTIR

(21) Mino, N.; Tamura, H.; Ogawa, K. *Langmuir* **1991**, *7*, 2336–2342.

(22) Deckert, A. A.; Fallon, L.; Kiernan, L.; Cashin, C.; Perrone, A.; Encalade, T. *Langmuir* **1994**, *10*, 1948–1954.

(23) Saito, A.; Urai, I.; Itoh, K. *Langmuir* **1996**, *12*, 3938–3944.

(24) Batchelder, D. N.; Bloor, D. *Advances in Infrared and Raman Spectroscopy*; Clark, R. J. H.; Hester, R. E., Eds.; Wiley: New York, 1984; Ch. 4.

(25) Smith, B. E. J.; Batchelder, D. N. *Polymer* **1991**, *32*, 1761–1769.

(26) Exarhos, G. L.; Risen, W. M.; Baughman, R. H. *J. Am. Chem. Soc.* **1976**, *98*, 481–487.

(27) Beckman, H. W.; Rubner, M. F. *Macromolecules* **1993**, *26*, 5192–5197.

(28) Tanaka, H.; Thakur, M.; Gomez, M. A.; Tonelli, A. E. *Macromolecules* **1987**, *20*, 3094–3097.

(29) Tanaka, H.; Gomez, M. A.; Tonelli, A. E.; Thakur, M. *Macromolecules* **1989**, *22*, 1208–1215.

(30) Chanoc, R. R. *Macromolecules* **1980**, *13*, 396–398.

(31) Rubner, M. F.; Sandman, D. J.; Velasquez, C. *Macromolecules* **1987**, *20*, 1296–1300.

(20) Peng, H.; Tang, J.; Chen, D.; Yang, L.; Ashbaugh, H. S.; Brinker, C. J.; Yang, Z.; Lu, Y. *J. Am. Chem. Soc.* **2005**, *127*, 12782–12783.

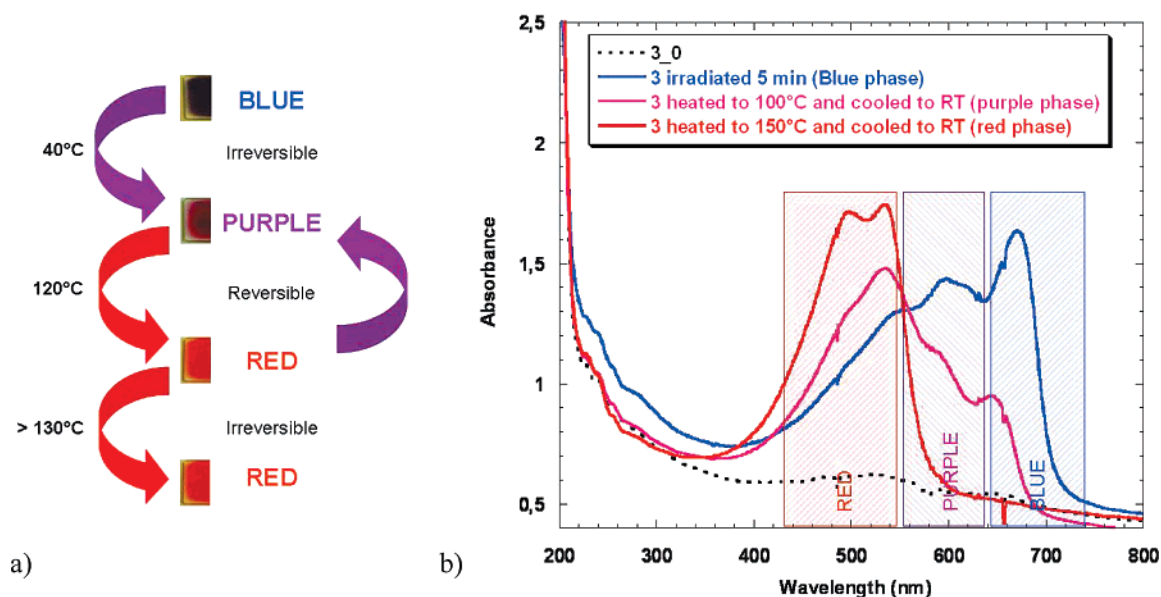


**Figure 6.** (a) Schematic diagram of thermochromic phases exhibited by **3** dropcast and irradiated on a quartz plate. (b) The three different UV–vis absorption spectra corresponding to the three different colors exhibited by **3** dropcast and irradiated on a quartz plate.

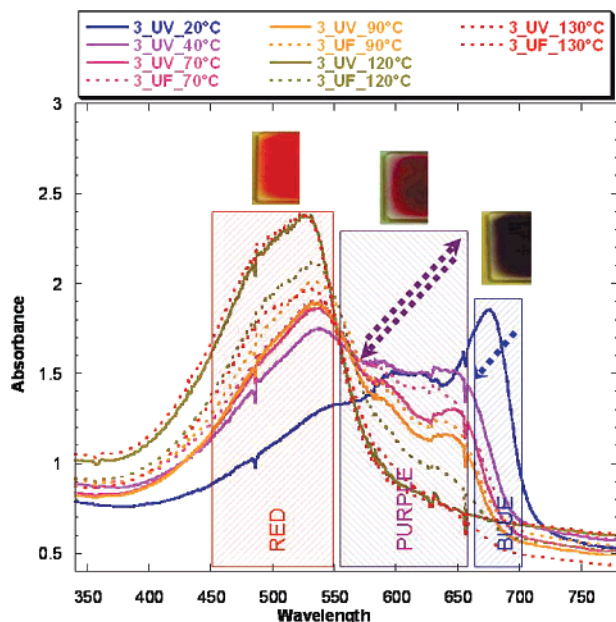


**Figure 7.** UV spectra as a function of temperature of a 2 mg/mL cyclohexane organogel of **3** dropcast between two quartz plates and irradiated once for 10 min at 254 nm at 20 °C prior to the first heating step. (Inset: photographs of the thermochromism exhibited by a glass plate covered by the organogel and irradiated for 10 min at 254 nm).

could readily provide information about specific urea groups and relative orientational transitions.<sup>32</sup>

In this context, using the same setup and the same sample, UV–vis and FTIR spectra were simultaneously recorded to highlight a relation between color changes and urea association mode changes (Figures 7–9). For that purpose, a 2 mg/mL cyclohexane organogel of **3** was dropcast between two slices of crystalline KBr in a sealed cell. This setup, described in the Supporting Information, is based on two crystalline KBr slices

transparent in the UV–vis and infrared wavelength range. It allowed the irradiation of the sample at 254 nm for 10 min at room temperature to produce the blue phase of PDA-**3**. The UV and FTIR spectra were recorded simultaneously. After its irradiation, the sample was heated stepwise (10 °C steps), and spectra were recorded at each step (spectra **3-UV-XX°C**). Between two temperature steps, the sample was cooled to room temperature, and the spectra were recorded (spectra **3-UF-XX°C**). Because of multiple reflections between the two slices of crystalline KBr, poor quality UV–vis spectra were obtained (see Supporting Information), so the UV–vis spectroscopic behavior of **3** was confirmed by the same experiment carried out between quartz plates (Figure 7).

#### Study of the Thermochromism by UV–vis Spectroscopy.

As shown by the UV measurements, the irradiation of the dropcast organogel of **3** between KBr slices furnished a blue film composed of three absorption bands with a maximum absorption at 675 nm (Figure 7, blue full line, inset: photographs of the thermochromism exhibited by a glass plate coated with the organogel and irradiated for 10 min at 254 nm). Upon heating to 40 °C, the band centered at 675 nm disappeared irreversibly, and the material adopted a purple color with an absorption band at 610 nm (Figure 7, spectrum **3-UV-40°C**). Heating the KBr cell up to 70 °C produced a red material with an absorption band at 530 nm (Figure 7, spectrum **3-UV-70°C**). Upon cooling to room temperature, the purple color was recovered showing the reversibility of this thermochromic phase (Figure 7, spectrum **3-UF-70°C**). Further heating in the temperature range of 70–120 °C produced a red color with a decrease in the reversibility of the thermochromism as the temperature increased (Figure 7, spectra **3-UV-90°C**, **3-UV-120°C**, **3-UF-90°C**, and **3-UF-120°C**, see also Supporting Information for intermediate temperatures). Finally, heating at and above 130 °C produced an irreversible red color (spectra **3-UV-130°C** and **3-UF-130°C**).

#### Study of the Thermochromism by FTIR Spectroscopy.

In a remarkable way, these thermochromic phases and their temperatures, characterized by UV–vis spectroscopy, could be

(32) Lio, A.; Reichert, A.; Ahn, D. J.; Nagy, J. O.; Salmeron, M.; Charych, D. H. *Langmuir* **1997**, *13*, 6524–6532.

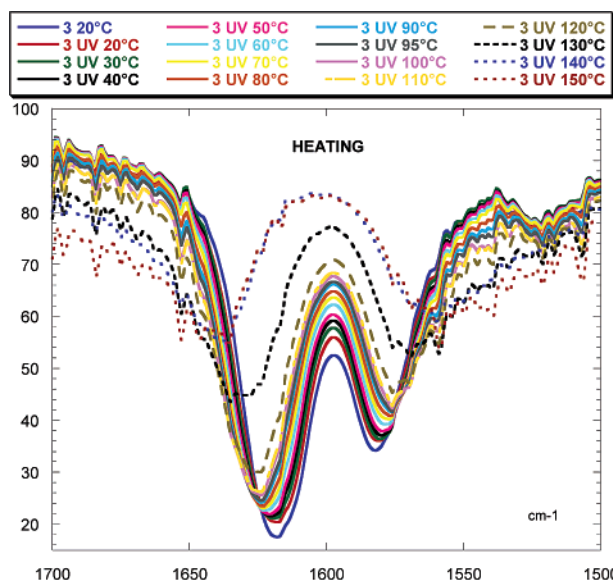


**Figure 8.** 3-UV-XX°C FTIR spectra recorded during heating of a 2 mg/mL cyclohexane organogel of **3** dropcast between two slices of crystalline KBr in a sealed cell and irradiated once for 10 min at 254 nm at 20 °C prior to the first heating step.

correlated to the hydrogen-bond strength and relative orientational transitions of the urea functions. Indeed, the FTIR spectra recorded simultaneously provided information about the wavenumbers, the intensities, and the shape of the Amide I and Amide II bands during heating and cooling (Figures 8 and 9). First, one can observe that the photopolymerization of **3** induced a slight modification of the hydrogen-bonded system. The Amide I band was shifted to higher wavenumber ( $\Delta\nu = +0.4 \text{ cm}^{-1}$ ), and the Amide II band was shifted to lower wavenumber ( $\Delta\nu = -0.7 \text{ cm}^{-1}$ ) (Figure 8, spectra **3-20°C** and **3-UV-20°C**). The intensities were decreased, and the bands were broadened. Those shifts, intensity, and shape modifications are significant to a less effective hydrogen bond. The contraction of the fiber backbone during the polymerization very slightly weakened the hydrogen-bonded network even in the presence of the aliphatic spacer. Second, heating from 20 to 150 °C modified the hydrogen-bonded system in the same trend, and like the UV-vis study, three phases could be discerned. From 20 to 120 °C, Amide I and Amide II are linearly shifted toward the free urea function with a crucial step at 120 °C. In the temperature range from 120 to 140 °C, heating had a dramatic effect on the hydrogen bond with highly shifted and intensity decreased Amide I and Amide II bands ( $\Delta\nu_{\text{AI}} = +20.7 \text{ cm}^{-1}$  and  $\Delta\nu_{\text{AII}} = -20.6 \text{ cm}^{-1}$ ) (Figure 8, spectra **3-UV-120°C**, **3-UV-130°C**, and **3-UV-140°C**). In the last phase, for temperatures above 140 °C, no further evolution of the hydrogen bond was noticed. Third, FTIR spectra recorded after cooling at each temperature step gave information about the reversibility of the thermally induced structural modifications (Figure 9).

From Figure 9, two types of structural modifications could be identified. For heating/cooling cycles below 120 °C, one can see clearly that the Amide I and Amide II bands recovered their wavenumbers, band intensities, and band shapes after cooling as attested by the spectra **3-UF-70°C** and **3-UF-120°C**, which matched perfectly the spectrum **3-UV-30°C** taken as a reference. This proves that the thermal deformations of the urea hydrogen-bond pattern and the structural modifications around the urea

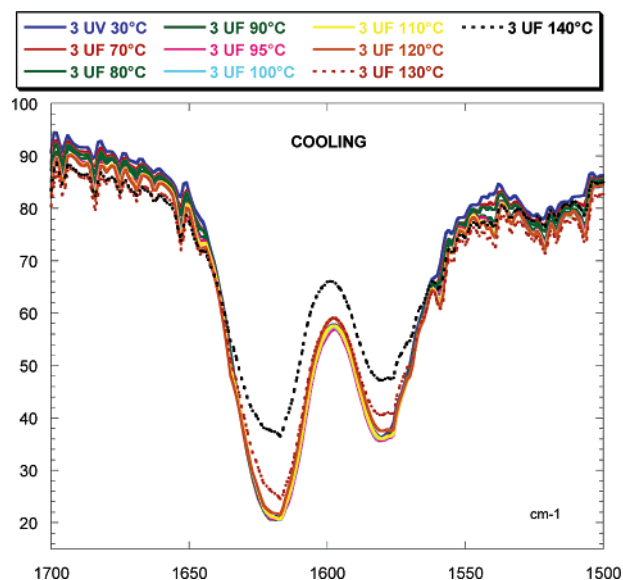


**Figure 9.** 3-UF-XX°C FTIR spectra recorded after each heating/cooling cycle of a 2 mg/mL cyclohexane organogel of **3** dropcast between two slices of crystalline KBr in a sealed cell and irradiated once for 10 min at 254 nm at 20 °C prior to the first heating step.

function are totally reversible. This range of temperature corresponds to the range of reversible thermochromism from purple to red observed by UV-vis spectroscopy and with the naked eye. For heating/cooling cycles realized above 120 °C, the FTIR band modifications are no longer reversible, and the urea functions must be involved in a new hydrogen-bonded network (Figure 9, spectra **3-UF-130°C** and **3-UF-140°C**). This new supramolecular organization produced irreversible modifications of the conjugated backbone being the origin of the observed irreversible red color. Again, no thermal alteration of the triethoxysilane functions was observed (see Supporting Information).

**Proposed Origin of the Structural Modifications.** Given the fact that short polymer diacetylene chains, like those obtained for **2**, also provide a red color, AFM measurements were realized on a 2 mg/mL cyclohexane organogel of **3** diluted 10-fold and dropcast on a silicon wafer before being irradiated and heated (see Supporting Information). Images were taken at each step of the generation of the red fibers on the same sample. Images, taken before the UV irradiation, after 10 min of irradiation at 254 nm at 20 °C and after heating/cooling cycles at 50, 70, and 130 °C confirm that long polymer fibers are still present even after the irreversible color change from purple to red at 130 °C. This result supports the role of the supramolecular reorganization in the thermochromic process. In this context, a schematic description of a possible mechanism for the molecular reorganization in the supramolecular fiber is represented in Figure 10. For reasons of clarity, the side chains in **3** were schematically simplified while respecting their sizes. The aliphatic parts were represented as black sticks and the triethoxysilane functions as black triangles.

From the AFM images, we can deduce that the polymeric fibers of 30–60 nm width are composed of 6 to 12 parallel single stacks of **3** (**3** width is  $\approx 5 \text{ nm}$ ). During the irradiation, fibers underwent a slight contraction (cf Figure 10, step A) due to the formation of the conjugated backbone as attested by the slight modification of the hydrogen-bond strength (cf. Figure



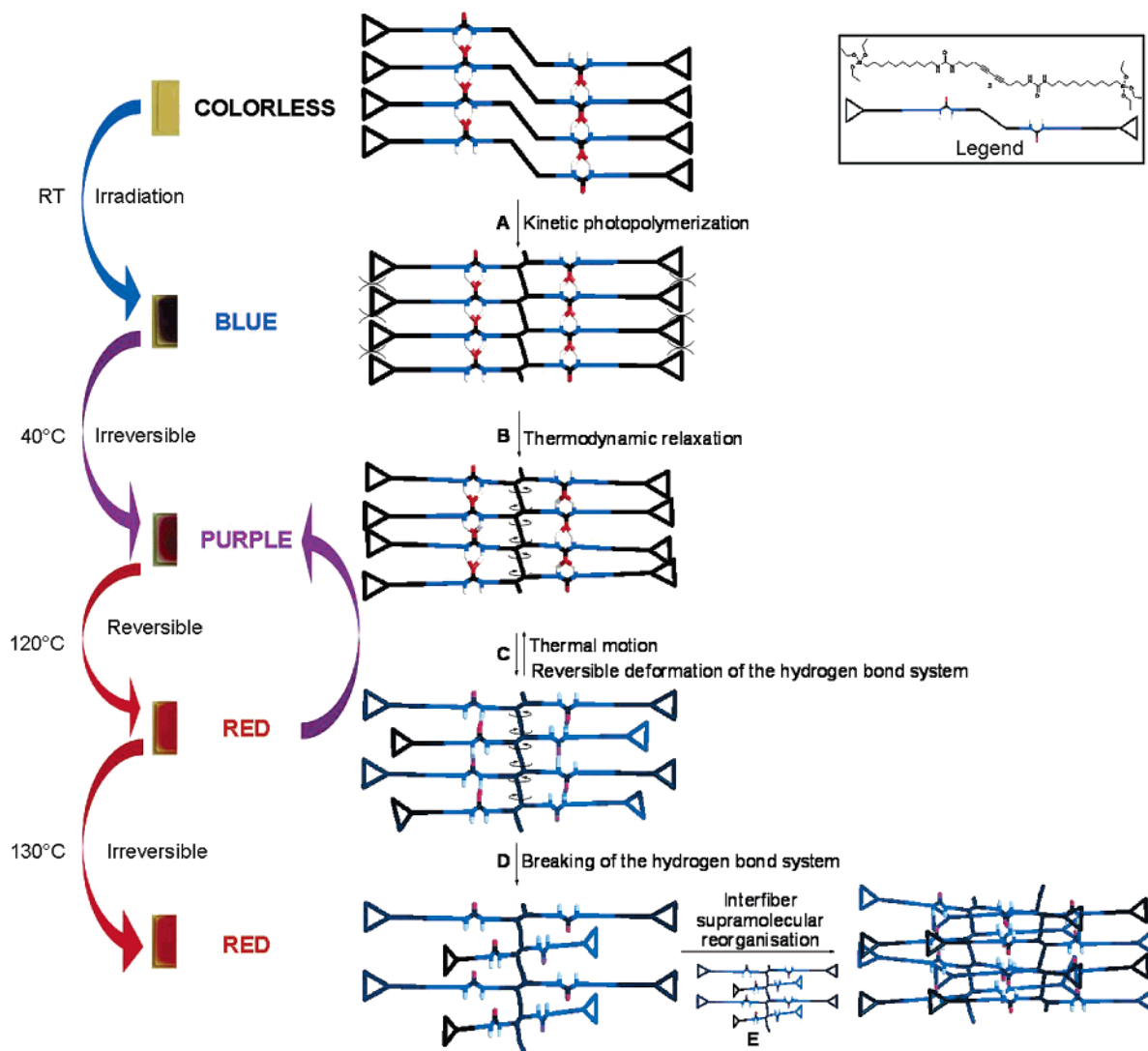


**Figure 10.** Schematic representation of the molecular organization in the supramolecular fiber in the different thermochromic phases exhibited by **3**.

8, spectra **3-20°C** and **3-UV-20°C**). This kinetically controlled reaction resulted in a blue PDA fiber. The steric hindrance introduced between side chains by the triethoxysilane functions could relax with a thermodynamic process during the first heating step ranging from room temperature to 40 °C (cf. Figure 10, step B). In this thermochromic phase (from blue to purple), even if the hydrogen-bond pattern is not modified (cf. Figure 8, spectra **3-UV-20°C**•••**3-UV-40°C**), the slight reorganization of the aliphatic side chains may produce a slight torsion of the aromatic backbone with a less effective conjugation. This thermodynamic relaxation is irreversible.

Further heating (from 40 to 150 °C) produced strong thermal motions of the side chains with a dramatic effect on the urea hydrogen-bond pattern and a strong torsion of the aromatic backbone producing a red color. From 40 to 120 °C, the hydrogen-bond modifications are reversible as attested by the FTIR study (cf. Figure 9, **3-UV-30°C** and **3-UF-70°C**•••**3-UF-120°C**). Indeed, the two hydrogen bonds defining the urea hydrogen-bond pattern are quite stable, and the cooperative effect of these two noncovalent interactions results in a reversible association/dissociation process of the motif even if one of them is weakened or broken (cf. Figure 10, step C). For temperatures higher than 130 °C, as attested by the FTIR study,

the hydrogen-bond modifications are no longer reversible. In this case, we believe that the two hydrogen bonds composing the urea hydrogen-bond pattern have been broken and rather than going back to a constrained situation, the urea self-associate with urea functions of a vicinal fiber (cf. Figure 10, steps D and E). This situation allowed the minimization of the steric interactions and the optimization of the hydrogen-bond formation. From Figure 9, it is clear that the hydrogen bond is less effective (Figure 9, spectra **3-UF-130°C** and **3-UF-140°C**, lower intensities and broader shapes of the Amide I and Amide II bands) but that the new supramolecular organization must be more stable with a better balance between attractive and repulsive forces.

#### Study of the Solvatochromism by UV–vis Spectroscopy.

The solvatochromism exhibited by the irradiated blue organogel of **3** is another indication of the different supramolecular interactions contributing to the different chromic transitions (Figure 11a). The addition of 1 mL of THF on top of the irradiated blue organogel (4 mg/mL in cyclohexane) and slow diffusion of this hydrogen-bond accepting solvent produced a chromic transition from blue to red. The color change is achieved by diffusion controlled exchange of solvent molecules. The gel state is retained, but syneresis produces a free handleable



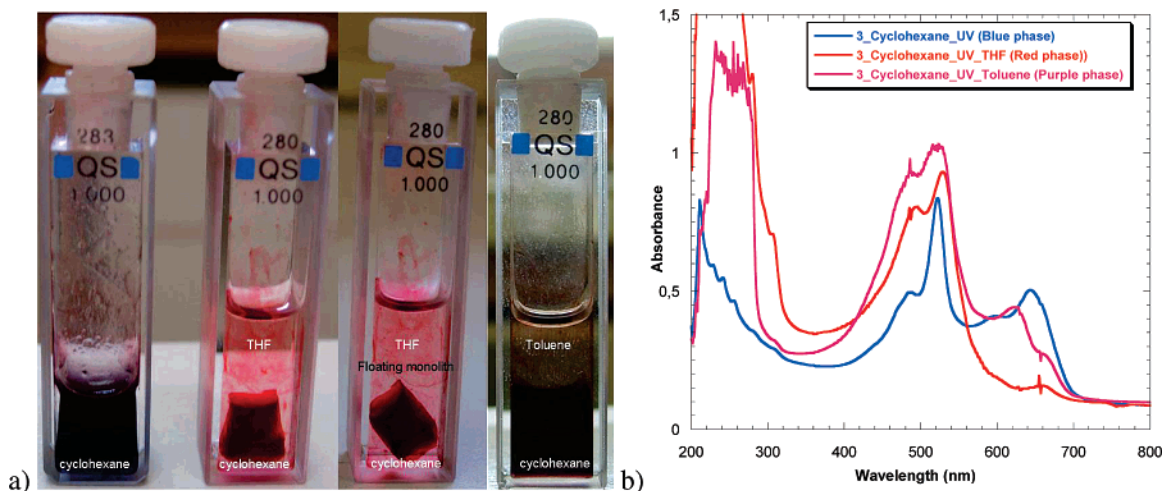


**Figure 11.** Solvatochromism of an organogel of **3** (4 mg/mL) in cyclohexane after 10 min of irradiation at 254 nm. Photographs (a) and UV-vis spectra (b) recorded before and after slow diffusion of THF or toluene.

PDA-OG monolith confirming that the long fibers maintain their integrity, thus stabilizing this supramolecular architecture. The syneresis could originate from the exchange of cyclohexane by THF, a smaller molecule, but also from the THF extraction of the nonpolymerized organogelator molecules trapped in the PDA-OG. The spectroscopic transition could be followed by UV-vis measurements (Figure 11b). FTIR spectroscopy does not show any modification of the hydrogen bond, but it confirmed that the triethoxysilane functions were unmodified (see Supporting Information). When the THF is replaced by toluene that is also a polar solvent but a hydrogen-bond nondonating and nonaccepting one, a purple phase was obtained, and the gel state was retained (Figure 11a). This polar solvent interacts with the polymer backbone through dipolar interactions, modifying its organization without hydrogen bond breaking. The resulting purple color corresponds to the irreversible color thermally obtained at 40 °C (cf. Figure 7, spectrum **3-UV-40°C**). This suggests that this irreversible thermochromic transition (blue to purple) was not the result of the modification of the hydrogen-bond network but a thermodynamic reorganization of the conjugated system. On the other hand, the urea function is really at the origin of the reversible character of the purple to red transition. Indeed, the two hydrogen bonds defining the urea hydrogen-bond pattern are very stable, and the cooperative effect of these two noncovalent interactions results in a reversible association/dissociation process of the motif even if one of them is weakened or broken.

**Study of the Acidochromism by UV-vis and FTIR Spectroscopies.** In the same manner, the contribution of the acido-catalyzed sol-gel process was revealed by the study of an organogel of **3** (4 mg/mL) in cyclohexane dropcast on a substrate and irradiated for 10 min at 254 nm. Films were either exposed or not to HCl vapors. Quartz plates were used for the study of the optical properties and silicon wafers for the studies related to the infrared spectroscopy. Pristine irradiated films will be noted as **3\_UV**. Those films submitted to the sol-gel process using HCl vapors will be noted as **3\_UV\_HCl**.

Upon exposition to HCl vapors of a blue thin film of **3** (Figure 12, blue lined spectrum) on a quartz plate, an acidochromic transition was observed. The absorption maximum hypsochromically shifted from 675 to 518 nm and the plate exhibited a red color.

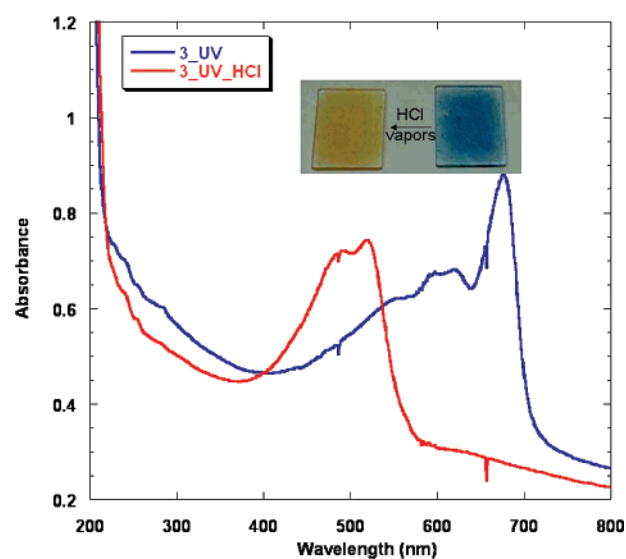


**Figure 12.** UV-vis spectra of an organogel of **3** (4 mg/mL) in cyclohexane dropcast on a quartz plate and irradiated for 10 min at 254 nm. Spectra recorded before (**3\_UV**) and after exposition to HCl vapors (**3\_UV\_HCl**). Inset: photographs of the quartz plates.

The hydrolysis polycondensation process could be monitored by infrared spectroscopy (Figure 13). During this chemical modification, the ethoxy groups of **3** were eliminated while Si-O-Si bonds were created. This transformation can be monitored from the band intensity of the asymmetric ( $\nu_{as}CH_3$ ) and symmetric ( $\nu_sCH_3$ ) stretching vibrations of the  $CH_3$  at, respectively, 2975 and 2883  $cm^{-1}$  (Figure 13a). In the FTIR spectrum of **3\_UV\_HCl**, these vibrations are absent, which is significant of the hydrolysis of the Si-OEt bonds. In the same way, the formation of the Si-O-Si network can be followed by the decrease of the band intensity of the asymmetric ( $\nu_{as}Si-O-CH_2$ ) and symmetric ( $\nu_sSi-O-CH_2$ ) stretching vibrations of the Si-O- $CH_2$  bond, observed at 1105 and 1079  $cm^{-1}$  (Figure 13b), respectively, and by the appearance of a broadband from 970 to 1180  $cm^{-1}$  corresponding to the asymmetric and symmetric stretching vibrations of the various Si-O-Si bonds of the silicate network. The condensation is complete after 20 min of thermal treatment at 110 °C. This was

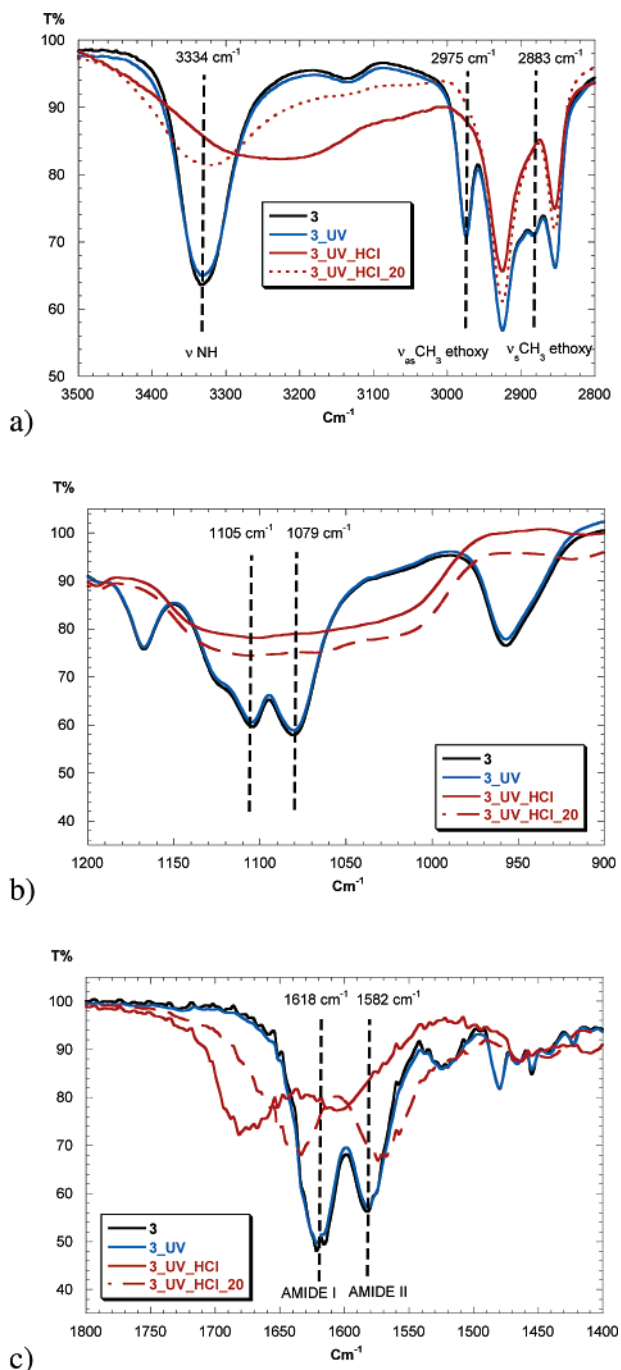


**Figure 13.** Infrared spectra of an organogel of **3** (4 mg/mL) in cyclohexane dropcast on a silicon wafer and irradiated for 10 min at 254 nm. Spectra recorded before (**3\_UV**) and after exposition to HCl vapor (**3\_UV\_HCl**). (a) Spectral region from 3500 to 2800  $\text{cm}^{-1}$ ; (b) spectral region from 1200 to 900  $\text{cm}^{-1}$ ; and (c) spectral region from 1800 to 1400  $\text{cm}^{-1}$ .

confirmed by the stability of the film **3\_UV\_HCl\_20** after washing with solvent.

Upon exposure of **3\_UV** thin films to HCl vapor, the Amide I and II bands were shifted to higher wavenumbers ( $\Delta\nu = +62$  and  $+32 \text{ cm}^{-1}$ , respectively) (Figure 13c, spectra **3\_UV\_HCl**). Intensities were decreased, and bands were broadened. Those shifts, intensity, and shape modifications are significant of free urea functions solvated by water or chlorine anions, being very strong hydrogen-bond acceptors. The same behavior was noticed for the absorption band corresponding to the N–H stretch ( $\nu_{\text{NH}}$

$= 3334 \text{ cm}^{-1}$ ). This band is broadened and shifted to lower wavenumbers by  $62 \text{ cm}^{-1}$ , and its intensity was decreased (Figure 13a, spectrum **3\_UV\_HCl**).

The thermal treatment also has a dramatic effect on the hydrogen bond. Indeed, this process results in the elimination of a hydrogen-bonded water and chlorine anion. The N–H band, shifted to low wavenumbers by the acid exposure, recovers its original position but stayed broad in shape and low in intensity. The Amide II band, shifted to higher wavenumbers by the acid exposure, was shifted to lower wavenumbers and remained broad in shape and low in intensity. Those spectroscopic modifications indicate a urea function engaged in a new supramolecular assembly. A correlation could be established with the final step observed in the thermochromism study. Indeed, both spectra (Figure 13c, spectrum **3\_UV\_HCl\_20** and Figure 9 spectrum **3-UF-140°C**) match perfectly, and in both cases, a modification of the supramolecular organization was envisaged. At this point, the red color is also irreversible.

## Conclusion

The introduction of the urea function as the structure directing agent of diacetylene organogels (DA-OGs) has been demonstrated. Ureido substituted diacetylenic organogelators were designed to achieve a balance between associative interactions and dispersion forces. Equilibrium between associative and dispersive forces was a requirement to reach the gel state without premature topochemical polymerization of the diacetylenic moiety. This role was played by the triethoxysilane end groups.

Depending on the length of the spacer chain ( $n$ ) between the polymerizable function and the urea of the ureido-organogelators, the photopolymerization of the organogels led to a loss of the gel state and small poorly conjugated red nano-objects ( $n = 1$ ) or a retention of the organogel and highly conjugated blue fibers ( $n = 3$ ).

Finally, the thermochromism exhibited by the highly conjugated ureido-polydiacetylene in the solid state was studied. The urea function and its perfectly defined hydrogen-bond pattern allowed us to establish a relationship between the results obtained from UV–vis and FTIR spectroscopies. The data led us to establish that the reversible thermochromic transition must be associated to a reversible supramolecular modification and conversely, irreversible chromic transitions are the result of irreversible structural modifications. In the same manner, effects of solvent and hydrolysis stimuli on the color of the nano-objects were also investigated. Correlations could be established between the different stimuli.

Until now, the one-dimensional supramolecular organization of diacetylene was related to the fabrication of electroconductive polydiacetylene fibers for nanoelectronic applications. We believe that the use of the diacetylene function, in addition to the electronic conductivity it brings, will offer also the possibility to isolate a single fiber. Indeed, we think that a single fiber could be isolated by dilution of supramolecular assemblies directed by weak bonds. However, these assemblies must be covalently stabilized before being diluted. A way to reach this goal is to reticulate the fiber in its center rather than at its extremities as it would be much easier through the use of Si-(OEt)<sub>3</sub> or acrylate groups. Indeed, this approach will lead in all cases to an interfiber cross-linking. Our approach, consisting

in the UV reticulation of a diacetylene core to obtain a polydiacetylene backbone seems very promising. This is the reason why we are currently focusing on the synthesis of functional bis-urea-diacetylenes by adjunction of functionality on the alkyl chains.

**Acknowledgment.** The authors gratefully acknowledge financial support from the Ministère de la Recherche (Action Concertée Nanosciences 2004) and the CNRS.

**Supporting Information Available:** Experimental procedures for the synthesis of **1–3** and **5–7**. Spectral data sets (NMR, UV–vis, FTIR, HRMS, and elemental analyses) and  $^1\text{H}$  and  $^{13}\text{C}$  NMR spectra for **2**, **3**, and **5–7**. Detailed experiments and full spectra for UV–vis and FTIR studies vs temperature. This material is available free of charge via the Internet at <http://pubs.acs.org>.

JA065434U